ARTICLE

Principles of Surface Potential Estimation in Mixed Electrolyte Solutions: Taking into Account Dielectric Saturation

Wen-xin Zou[a], Jing Peng[a], Wei-ning Xiu[b], Xin-min Liu[a*]

a. Chongqing key Laboratory of Soil Multi-scale Interfacial Process, College of Resources and Environment, Southwest University, Chongqing 400715, China
b. Institute of Agricultural Engineering, Chongqing Academy of Agricultural Sciences, Chongqing 401329, China

(Dated: Received on July 6, 2019; Accepted on September 19, 2019)

The dielectric properties between in-particle/water interface and bulk solution are significantly different, which are ignored in the theories of surface potential estimation. The analytical expressions of surface potential considering the dielectric saturation were derived in mixed electrolytes based on the nonlinear Poisson-Boltzmann equation. The surface potentials calculated from the approximate analytical and exact numerical solutions agreed with each other for a wide range of surface charge densities and ion concentrations. The effects of dielectric saturation became important for surface charge densities larger than 0.30 C/m^2. The analytical models of surface potential in different mixed electrolytes were valid based on original Poisson-Boltzmann equation for surface charge densities smaller than 0.30 C/m^2. The analytical model of surface potential considering the dielectric saturation for low surface charge density can return to the result of classical Poisson-Boltzmann theory. The obtained surface potential in this study can correctly predict the adsorption selectivity between monovalent and bivalent counterions.

Key words: Dielectric property, Electrical double layer, Surface charge, Colloid particle

I. INTRODUCTION

The surface potential plays an important role in the solid/liquid interfacial interactions, it is an important electrochemical property in the colloidal system that controls the colloidal particles interaction. The electrical double layer (EDL) is normally described using the Poisson-Boltzman (PB) model and play a central role in many interfacial phenomena [1]. However, an important property of EDL that still remains poorly understood is the surface potential [2].

The existing theories and methods for estimating surface potential of charged particles in electrolyte solutions are based on the second harmonic generation [3, 4], classical PB equation [5−7], X-ray photoelectron spectroscopy [2], and electrokinetic (zeta) potential [8]. Although most current studies use the zeta potential as an alternative to the surface potential, zeta potential is obviously lower than the surface potential [9]. The effects of the electric field on the dielectric property at the particle/water interface were neglected in the surface potential based on the EDL theory. The surface charges of nano/colloidal particles can generate strong electric field [10], which is nonlinear descent as the distance from the surface increases, and thus the solid/liquid interface cannot be seen as homogeneous dielectric system [11, 12]. Similarly, the second harmonic method for measuring surface potential is still based on the Gouy-Chapman model and does not consider the influences of the dielectric decrement. Therefore, a theory for the surface potential measurement considering dielectric saturation is important to correctly estimate solid/liquid interfacial properties and interactions. It should be mentioned that the surface potential is the potential of original plane of the diffuse layer (or Stern potential) in this study since the effects of hydrated cation size are neglected, *i.e.* without considering thickness of the Stern layer.

The dielectric decrement in a strong electrostatic field [13−15] further enhances the complexation of charged ions into neutral species [16, 17]. In a study devoted to the effect of dielectric saturation on the EDL structure, Grahame proposed the application of an empirical equation to describe the relationships between the dielectric constant and the electric field strength [18]. If the electric field strength was less than 2.56×10^8 V/m, the effects of dielectric saturation and ionic polarization (opposite in sign) can almost balance each other [19]. Actually, however, the electric field always exceeds 2.56×10^8 V/m, implying the dielectric saturation may become more important than the ionic polarization (resulting from weak quantum fluctuations) [9]. Large

*Author to whom correspondence should be addressed. E-mail: lxm2016@swu.edu.cn, Tel.:+86-23-68251249

doping densities of graphene were found to be related to large potential drops across the EDL [20], which gives rise to significant dielectric saturation in the electrolyte solutions [12, 21−23]. Although dielectric saturation is only important within the first hydration shell of the ion, it is non-negligible for ions in water [24]. The dielectric saturation of water strongly affects the EDL capacitance of an electrolytically top-gated graphene due to the strong electric field near the surface [20, 25, 26]. Therefore, the electrical potential and structure of EDL can be strongly affected by the dielectric saturation at the charged interfaces.

In practical applications, the interfacial reactions usually occur under the mixed electrolyte solutions. Although the methods of surface potential measurement have developed from a simple single electrolyte [5] to complicated mixed electrolytes [7], surface potential is also underestimated owing to the neglect of the dielectric saturation [27]. The theory to determine surface potential has been derived with consideration of the dielectric saturation in single electrolyte solutions [28]. In the present study, the analytical model of surface potential measurement considering the dielectric saturation in the mixed electrolytes was proposed using a mean-field description of the system by solving the nonlinear PB equation.

II. SURFACE POTENTIAL CALCULATED FROM NUMERICAL SOLUTION

Based on the Boltzmann equation, the distribution of ion concentration at the solid/liquid interface can be expressed as:

$$f_i(x) = f_i \mathrm{e}^{-Z_i F\varphi(x)/(RT)} \tag{1}$$

where f_i (in mol/dm^3) is the concentration of ith ion in the bulk solution, Z_i is the valence of the ith ions, F (in C/mol) is the Faraday constant, $\varphi(x)$ (in V) is the potential distribution in the diffuse layer, R (in J·mol^{-1}·K^{-1}) is the gas constant, and T (in K) is the absolute temperature.

For a planar wall of the diffuse layer, the Poisson equation can be expressed as:

$$\frac{\mathrm{d}\left(D\dfrac{\mathrm{d}\varphi}{\mathrm{d}x}\right)}{\mathrm{d}x} = -\frac{\rho(x)}{\varepsilon_0} \tag{2}$$

where ε_0 (in C^2·J^{-1}·dm^{-1}) is the vacuum dielectric constant, D is the relative dielectric function of medium, $\rho(x)$ (in C/dm^3) is the volumetric charge density distribution in EDL and $\rho(x)=\sum Z_i F f_i(x)$. Therefore, Eq.(2) can be changed as PB equation:

$$\frac{\mathrm{d}\left(D\dfrac{\mathrm{d}\varphi}{\mathrm{d}x}\right)}{\mathrm{d}x} = -\frac{1}{\varepsilon_0}\sum Z_i F f_i \mathrm{e}^{-Z_i F\varphi(x)/(RT)} \tag{3}$$

We assume that the diffuse layers of two particles will not overlap, and the boundary conditions subject to Eq.(3) are given by:

$$\left.\frac{\mathrm{d}\varphi}{\mathrm{d}x}\right|_{x=+\infty} = 0 \tag{4}$$

$$\varphi(x)|_{x=+\infty} = 0 \tag{5}$$

Eq.(3) can be written as:

$$2E\mathrm{d}(DE) = -\frac{2}{\varepsilon_0}\sum Z_i F f_i \mathrm{e}^{-Z_i F\varphi/(RT)}\mathrm{d}\varphi \tag{6}$$

where E=−dφ/dx (in V/dm) represents electric field distribution in the diffuse layer, which is a function of distance x from surface. Therefore, Eq.(6) can be integrated as:

$$\int_0^{D(x)E(x)} 2E\mathrm{d}(DE) = \frac{2RT}{\varepsilon_0}\sum_i f_i\left(\mathrm{e}^{-Z_i F\varphi(x)/(RT)} - 1\right) \tag{7}$$

The left side of Eq.(7) can be rewritten as:

$$\int_0^{D(x)E(x)} 2E\mathrm{d}(DE) = 2D(x)E^2(x) - \int_0^{E^2(x)} D\mathrm{d}E^2 = g(E_x) \tag{8}$$

where $g(E_x)$ (in V^2/dm^2) is some function of $E(x)$, $D(x)$=$D(E(x))$ is actually a function of $E(x)$.

Besides imposing the continuity of the electric potential, we also require that the electrostatic jump conditions for the electric field $E(x)$=−dφ/dx are satisfied at x=0 and x=+∞. Assuming zero electric field in the region x<0, we have at the particle surface (Stern plane in this study x=0) [20]:

$$\varepsilon_0 D(0)E(0) = -\sigma(0) \tag{9}$$

where $E(0)\equiv E_0$, $D(0)\equiv D(E_0)=D_0$ and $\sigma(0)\equiv\sigma_0$ are the relative dielectric permittivity, the electric field strength, and the charge density at particle surface, respectively.

Therefore, Eq.(8) can be written as:

$$g(E_0) = 2D_0{E_0}^2 - \int_0^{{E_0}^2} D\mathrm{d}E^2 \tag{10}$$

at x=0 and then Eq.(7) can be written correspondingly as:

$$g(E_0) = \frac{2RT}{\varepsilon_0}\sum_i f_i\left(\mathrm{e}^{-Z_i F\varphi_0/(RT)} - 1\right) \tag{11}$$

To include the effects of water orientation polarization and variation in dielectric permittivity in a local

DOI:10.1063/1674-0068/cjcp1907132

electric field on the electrostatic potential, a nonlinear dielectric function is given by [29, 30]:

$$D = D_{\rm v} + \frac{f_{\rm w} p_{\rm w}}{\varepsilon_{\rm v} E} L\left(\frac{p_{\rm w} E}{kT}\right) \tag{12}$$

where the Langevin function $L(u)$=coth$u$−1/u. $D_{\rm v}$=1 is the relative dielectric permittivity of vacuum, $f_{\rm w}$ is the dipolar fluid of concentration (*i.e.*, water in this study), $p_{\rm w}$ is the molecular dipole moment of water.

In the limit of a constant for a vanishing electric field, E→0, Eq.(12) reduces to an effective homogeneous dielectric constant

$$D_{\rm w} = 1 + \frac{{p_{\rm w}}^2 f_{\rm w}}{(3\varepsilon_{\rm v} kT)} \tag{13}$$

Taking account of the dielectric response of molecules with intrinsic dipoles in dilute systems is well known, and a fitted parameter of $p_{\rm w}$=4.86 Debye was chosen, so $D_{\rm w}$=80 for $f_{\rm w}$=55 mol^{-1} at room temperature [17]. The Langevin equation given by Abrashkin *et al.* [17] reflects in the predicted increase of D values near the charged surface, which is not possible [29]. Therefore, the Langevin equation given by Eq.(12) is selected in the present study.

The integral of Eq.(10) with Eq.(12) is mathematically invalid based on the analyses in our previous studies [14, 28], an equivalent dielectric function with Grahame model is given by [18]:

$$D = D_{\rm v} + \frac{D_{\rm w} - D_{\rm v}}{\sqrt{1 + n\left(\frac{p_{\rm w} E}{kT}\right)^2}} \tag{14}$$

where $D_{\rm v}$ is relative dielectric constant of vacuum, the $p_{\rm w}/(kT)$=3.94×10^{-9} m/V at T=298 K, $D_{\rm w}$=1+${p_{\rm w}}^2 f_{\rm w}/(3\varepsilon_{\rm v} kT)$ is the relative dielectric constant of water in the bulk solution and $D_{\rm w}$=80. The original Grahame model [18] is an empirical equation because the parameter depends on experimental results. In the present study, the parameter n can be estimated theoretically. Based on Eq.(12) and Eq.(14), one has:

$$n = \frac{1}{\left[3L\left(\frac{p_{\rm w} E}{kT}\right)\right]^2} - \frac{1}{\left(\frac{p_{\rm w} E}{kT}\right)^2} \tag{15}$$

Eq.(15) shows that n=0 for E→0, n=0.133 for E=2.5×10^5→2.5×10^9 V/m and n=0.133→0.114 for E=2.5×10^9→2.5×10^{10} V/m. If the electric field is evaluated, the dielectric constant at the surface can be calculated by Eq.(14).

Introducing Eq.(14) into Eq.(9), we have:

$$-\frac{\sigma_0}{E_0 \varepsilon_0} = D_{\rm v} + \frac{D_{\rm w} - D_{\rm v}}{\sqrt{1 + n\alpha^2 {E_0}^2}} \tag{16}$$

here α=$p_{\rm w}/kT$. σ_0=1.8×10^{-4} C/m^2 with E=2.5×10^5 V/m and σ_0=0.72 C/m^2 with E=2.5×10^{10} V/m. The surface charge densities of many materials are within this range. An average value n=[0.133+(0.133+0.114)/2]/2=0.128 is selected for charged surface with different charge densities, based on the results of Eq.(15).

The dielectric decrement in the diffuse layer depends on the electric field strengths or charge densities based on the above theoretical calculations. Therefore, the charge density in Eq.(16) can reflect the contributions of material properties to dielectric saturation.

Introducing Eq.(14) into Eq.(10), one has:

$$g(E_0) = \frac{2{E_0}^2 (D_{\rm w} - 1)}{\sqrt{1 + n\alpha^2 {E_0}^2}} - \frac{2(D_{\rm w} - 1)}{n\alpha^2}\left(\sqrt{1 + n\alpha^2 {E_0}^2} - 1\right) + {E_0}^2 \tag{17}$$

when E_0→0, Eq.(17) returns to the result of classical PB theory, *i.e.* $g(E_0)$=$D_{\rm w}{E_0}^2$.

Introducing Eq.(17) into Eq.(11), we have:

$$\frac{2{E_0}^2 (D_{\rm w} - 1)}{\sqrt{1 + n\alpha^2 {E_0}^2}} - \frac{2(D_{\rm w} - 1)}{n\alpha^2}\left(\sqrt{1 + n\alpha^2 {E_0}^2} - 1\right) + {E_0}^2 = \frac{2RT}{\varepsilon_0}\sum_i f_i \left(\mathrm{e}^{-Z_i F\varphi_0/(RT)} - 1\right) \tag{18}$$

Eq.(18) is the theoretical expression of surface potential. Once the charge density is determined in advance, the electric field can be evaluated by Eq.(16), and then the surface potential can be determined by Eq.(18) using the numerical solutions in different mixed electrolytes. It should be noted that the theoretical derivation in this study based on the assumptions of a planar wall of diffuse layer and point-like ions. The effects of dielectric decrement were taken into account for point-like ions, while an assumption of homogeneous medium was used in classical theories.

Specially, when the dielectric saturation is neglected, *i.e.* classical Gouy-Chapman model, Eq.(18) can be changed as:

$$D_{\rm w}{E_0}^2 = \frac{2RT}{\varepsilon_0}\sum_i f_i \left(\mathrm{e}^{-Z_i F\varphi_0/(RT)} - 1\right) \tag{19}$$

$$\frac{{\sigma_0}^2}{\varepsilon_0 D_{\rm w}} = 2RT\sum_i f_i \left(\mathrm{e}^{-Z_i F\varphi_0/(RT)} - 1\right) \tag{20}$$

where E_0=$\sigma_0/(\varepsilon_0 D_{\rm w})$.

III. SURFACE POTENTIAL CALCULATED FROM ANALYTICAL SOLUTIONS

Although Eq.(18) can be used to estimate numerically the surface potential, the calculations are complex. In addition, the establishment of some analytical theories, such as ion adsorption/desorption and EDL interactions *etc.*, requires an analytical expression of the surface potential, especially in mixed electrolyte solutions.

DOI:10.1063/1674-0068/cjcp1907132

We use the following three mixed electrolyte solutions as examples.

A. Surface potential in 1:1+2:2 mixed electrolytes

For 1:1 (AB) and 2:2 (CD) mixed electrolyte solutions, Eq.(18) can be rewritten as:

$$\begin{aligned} & f_{\mathrm{A}}\mathrm{e}^{-F\varphi_0/(RT)} + f_{\mathrm{A}}\mathrm{e}^{F\varphi_0/(RT)} + f_{\mathrm{C}}\mathrm{e}^{-2F\varphi_0/(RT)} + \\ & f_{\mathrm{C}}\mathrm{e}^{2F\varphi_0/(RT)} \\ = & \frac{\varepsilon_0 g\,(E_0)}{2RT} + 2(f_{\mathrm{A}} + f_{\mathrm{C}}) \\ = & m_1 \end{aligned} \tag{21}$$

where f_{A} and f_{C} are the concentrations of the Ath and Cth ion species in the bulk solution.

If

$$\frac{f_{\mathrm{A}}\mathrm{e}^{3F\varphi_0/(RT)}}{f_{\mathrm{C}}\mathrm{e}^{3F\varphi_0/(RT)} + f_{\mathrm{A}}\mathrm{e}^{2F\varphi_0/(RT)} - m_1\mathrm{e}^{F\varphi_0/(RT)} + f_{\mathrm{A}}} \leq 5\%,$$

i.e. Eq.(21) can be changed as:

$$\varphi_0 = \frac{RT}{F}\ln\left(\frac{f_{\mathrm{A}} + \sqrt{{f_{\mathrm{A}}}^2 + 4m_1 f_{\mathrm{C}}}}{2m_1}\right) \tag{22}$$

Especially, when $f_{\mathrm{A}}{=}f_{\mathrm{C}}{=}f$ and $m_1{=}\dfrac{\varepsilon_0 g\,(E_0)}{2RT}{+}4f$, Eq.(22) can be changed as:

$$\varphi_0 = \frac{RT}{F}\ln\left(\frac{f + \sqrt{f^2 + 4m_1 f}}{2m_1}\right) \tag{23}$$

Eq.(22) and Eq.(23) are the analytical expressions of surface potential in 1:1+2:2 mixed electrolytes.

B. Surface potential in 1:1+1:2 mixed electrolytes

For 1:1 (AB) and 1:2 ($\mathrm{E_2J}$) mixed electrolyte solutions, Eq.(18) can be rewritten as:

$$\begin{aligned} & (f_{\mathrm{A}} + 2f_{\mathrm{J}})\mathrm{e}^{-F\varphi_0/(RT)} + f_{\mathrm{A}}\mathrm{e}^{F\varphi_0/(RT)} + f_{\mathrm{J}}\mathrm{e}^{2F\varphi_0/(RT)} \\ = & \frac{\varepsilon_0 g\,(E_0)}{2RT} + 2f_{\mathrm{A}} + 3f_{\mathrm{J}} \\ = & m_2 \end{aligned} \tag{24}$$

where f_{J} are the concentrations of the Jth ion species in the bulk solution.

Eq.(24) is a theoretical expression of the surface potential of 1:1+1:2 mixed electrolyte solutions, which is a function of the electric field considering the dielectric saturation.

If

$$(f_{\mathrm{J}}\mathrm{e}^{2F\varphi_0/(RT)})/(f_{\mathrm{J}}\mathrm{e}^{2F\varphi_0/(RT)} + f_{\mathrm{A}}\mathrm{e}^{F\varphi_0/(RT)} - m_2) \leq 5\%,$$

i.e. Eq.(24) can be changed as:

$$\varphi_0 = \frac{RT}{F}\ln\left(\frac{m_2 - \sqrt{{m_2}^2 - 4f_{\mathrm{A}}(f_{\mathrm{A}} + 2f_{\mathrm{J}})}}{2f_{\mathrm{A}}}\right) \tag{25}$$

Especially, when $f_{\mathrm{A}}{=}f_{\mathrm{J}}{=}f$ and $m_2{=}\dfrac{\varepsilon_0 g\,(E_0)}{2RT}{+}5f$, Eq.(24) can be changed as:

$$\varphi_0 = \frac{RT}{F}\ln\left(\frac{m_2 - \sqrt{{m_2}^2 - 12f^2}}{2f}\right) \tag{26}$$

C. Surface potential in 1:1+2:1 mixed electrolytes

For 1:1 (AB) and 2:1 ($\mathrm{GH_2}$) mixed electrolyte solutions, Eq.(18) can be rewritten as:

$$\begin{aligned} & f_{\mathrm{A}}\mathrm{e}^{-F\varphi_0/(RT)} + (f_{\mathrm{A}} + 2f_{\mathrm{G}})\mathrm{e}^{F\varphi_0/(RT)} + f_{\mathrm{G}}\mathrm{e}^{-2F\varphi_0/(RT)} \\ = & \frac{\varepsilon_0 g\,(E_0)}{2RT} + 2f_{\mathrm{A}} + 3f_{\mathrm{G}} \\ = & m_3 \end{aligned} \tag{27}$$

where f_{G} are the concentrations of the Gth ion species in the bulk solution.

Eq.(27) is a theoretical expression of the surface potential in 1:1+2:1 mixed electrolyte solutions, which is also a function of the electric field considering the dielectric properties.

If

$$\frac{(f_{\mathrm{A}} + 2f_{\mathrm{G}})\mathrm{e}^{2F\varphi_0/(RT)}}{(f_{\mathrm{A}} + 2f_{\mathrm{G}})\mathrm{e}^{2F\varphi_0/(RT)} - m_3\mathrm{e}^{F\varphi_0/(RT)} + f_{\mathrm{A}}} \leq 5\%,$$

i.e. Eq.(27) can be changed as:

$$\varphi_0 = \frac{RT}{F}\ln\left(\frac{f_{\mathrm{A}} + \sqrt{{f_{\mathrm{A}}}^2 + 4m_3 f_{\mathrm{G}}}}{2m_3}\right) \tag{28}$$

Especially, when $f_{\mathrm{A}}{=}f_{\mathrm{G}}{=}f$ and $m_3{=}\dfrac{\varepsilon_0 g\,(E_0)}{2RT}{+}5f$, Eq.(27) can be changed as:

$$\varphi_0 = \frac{RT}{F}\ln\left(\frac{f + \sqrt{f^2 + 4m_3 f}}{2m_3}\right) \tag{29}$$

The above analytical equations for surface potential in different mixed electrolytes were derived through some approximate conditions. The subsequent discussion would be focused on the validity of the analytical relations for the surface potential.

IV. COMPARISONS OF SURFACE POTENTIALS BETWEEN NUMERICAL AND ANALYTICAL EQUATIONS

The colloidal particle interactions [31] and ion exchange adsorption [32, 33] strongly depend on surface

DOI:10.1063/1674-0068/cjcp1907132

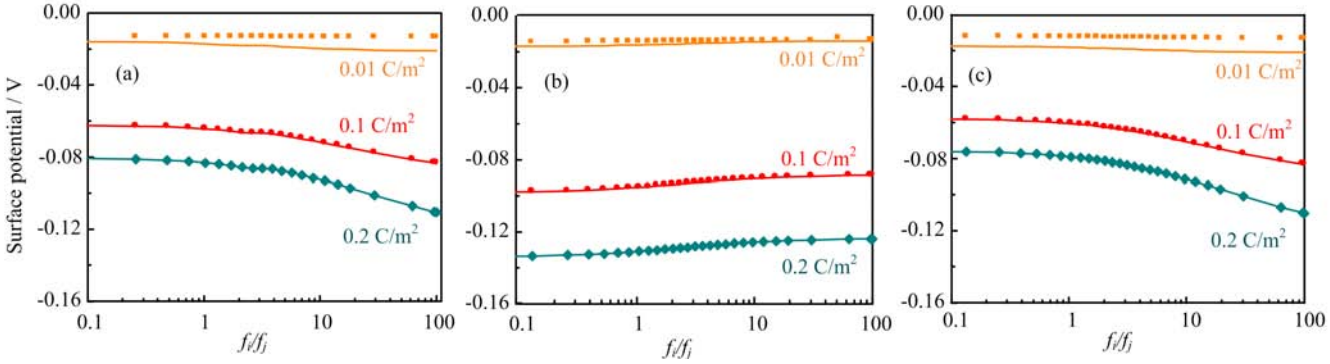

FIG. 1 The relationships between ion concentration ratio and surface potential in (a) 1:1+2:2, (b) 1:1+1:2 and (c) 1:1+2:1 electrolyte solutions. The symbols represent numerical surface potential and the solid lines represent analytical surface potential, f_i/f_j is the ratio of bivalent ion concentration in mixed electrolytes with 0.1 mol/L ion strength.

potential. A reliable analytical expression of the surface potential can greatly simplify the calculation procedure.

FIG. 1 shows the surface potentials in the 1:1+2:2, 1:1+1:2 and 1:1+2:1 mixed electrolytes as a function of concentration ratio f_i/f_j at 0.1 mol/L ion strength, respectively. The surface potentials in 1:1+2:2 (FIG. 1(a)) and 1:1+2:1 (FIG. 1(c)) electrolytes have followed a similar trend. The surface potential values of the former are slightly larger than those of the latter, indicating that the surface potential of negatively charged particles is mainly determined by cations in solutions. The surface potentials increase with increasing f_i/f_j in the bulk solution and surface charge density, and their changes for f_i/f_j=0.1 are less than those for f_i/f_j=100. This is because the concentration of divalent cations relatively decreases with increasing f_i/f_j, and the screening of surface charge weakens. When f_i/f_j is very small, the divalent cations play a major role, the charge shielding is similar under the same ionic strength, thus the surface potential does not greatly change. In the 1:1+1:2 electrolyte solution, the counterions are also monovalent (FIG. 1(b)), the surface potentials for different charge densities are higher than those in the other two electrolytes. It is worth mentioning that only the ion-surface Coulomb interactions are taken into account based on the classical EDL theory in present study. In the subsequent study, we will further establish a theoretical model for surface potential measurement considering both specific ion effects and dielectric saturation.

The surface potentials obtained by the analytical and numerical solutions are in agreement with each other for a relative high charge density. The difference between the approximate (analytical) and the exact (numerical) surface potentials increases with decreasing surface charge density and increasing f_i/f_j values in the 1:1+2:2 and 1:1+2:1 electrolytes (FIG. 1 (a) and (c)). The relative error is large only for a very low charge density (*e.g.* 0.01 C/m^2 in FIG. 1). The surface charge densities of materials are usually larger than 0.01 C/m^2, therefore, the analytical expression can obtain the correct surface potentials in practical applications.

The electric field strength in the diffuse layer was strongly affected by the f_i/f_j values between bivalent and monovalent counterions [10]. For a large f_i/f_j value, there are more ith and less jth species ions distributed in the inner space of the diffuse layer. If the valences of ith and jth counterions are equal, their distribution in the diffuse layer does not affect the electric field strength and surface potential (FIG. 1(b)). However, surface potentials are strongly affected by the distribution for counterions with different valences, (FIG. 1 (a) and (c)).

FIG. 2 shows the surface potentials in the 1:1+2:2, 1:1+1:2 and 1:1+2:1 mixed electrolytes as a function of counterion concentration, respectively. The surface potentials calculated from the numerical and analytical solution in 1:1+2:2 (FIG. 2(a)) and 1:1+2:1 electrolytes (FIG. 2(c)) agree well with each other for 0.1 and 0.2 C/m^2, respectively. The difference between them increases with increasing counterionic concentration only at >0.016 mol/L for 0.01 C/m^2. The correct surface potential can be obtained from the analytical expression in practical applications for many materials. It also shows that the concentrations of counterions mainly determine the surface potential. In 1:1+1:2 electrolytes (FIG. 2(b)), the monovalent counterion weakly screens charges and then results in the high potential, and the difference between the analytical and numerical results is small. In the pure-solvent case (zero electrolyte concentration), it follows from electrostatic continuity conditions that difference of electric potentials between the two phases is identically zero. In the case of dilute electrolyte solutions, however, the difference of electric potentials is no longer equal to zero [34]. Since all real polar solvents are ionized to some extent, this effect should be taken into account in determining surface potential in experiments.

Bolt used illite as a material and studied the ion exchange equilibrium under a wide range of concentrations and Na/Ca concentration ratios in NaCl+$CaCl_2$

DOI:10.1063/1674-0068/cjcp1907132

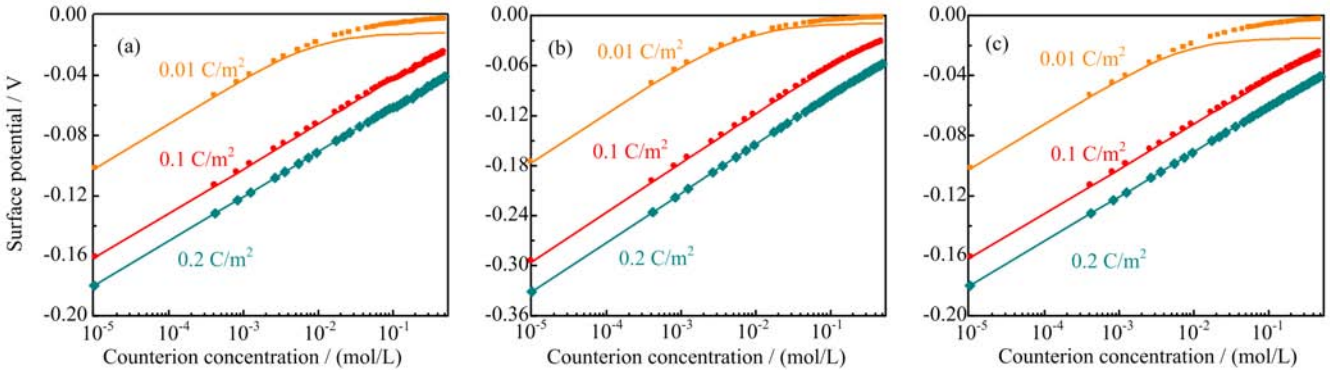

FIG. 2 The relationships between ion concentration and surface potential in (a) 1:1+2:2, (b) 1:1+1:2 and (c) 1:1+2:1 electrolyte solutions as f_i=f_j in different surface charge densities. The symbols represent numerical surface potential and the solid lines represent analytical results.

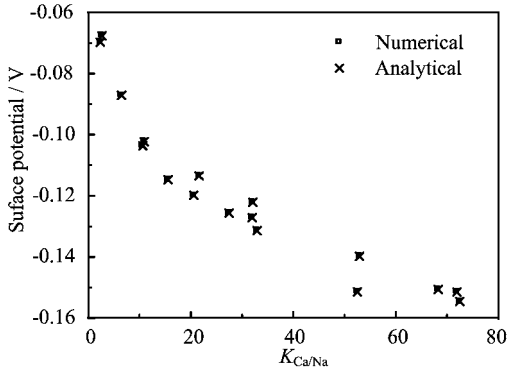

FIG. 3 Surface potential of illite particle in NaCl+$CaCl_2$ electrolytes, the numerical and analytical results are calculated using Eq.(26) and Eq.(27), respectively. $K_{Ca/Na}$ (=$f_{Na}N_{Ca}/(f_{Ca}N_{Na})$) is selectivity coefficient, f_{Na} and f_{Ca} are concentrations of Na^+ and Ca^{2+} in bulk solutions, N_{Na} and N_{Ca} are adsorption amount of Na^+ and Ca^{2+}, respectively. The surface charge density of illite particle is 0.2895 C/m^2, the concentrations of Na^+ and Ca^{2+} were determined by the binary Na-Ca exchange equilibrium on illite surface [35].

(1:1+2:1) mixed system [35]. Surface charge density of illite (0.2895 C/m^2) was measured using a negative adsorption method, the electric field strength corresponds to 5.15×10^8 V/m. The exact numerical and approximate analytical solutions of the surface potential can be calculated from Eq.(27) and Eq.(28), respectively. The relative error with less than 1% indicates that the analytical expression of the surface potential is valid (FIG. 3).

The surface potentials in the mixed solutions of 1:1+2:2 (FIG. 4(a)) and 1:1+2:1 (FIG. 4(c)) electrolytes follow a similar trend. The difference between the exact and the approximate surface potentials also increases with decreasing surface charge density and increasing f_i/f_j values. In the 1:1+1:2 electrolyte solution, the surface potentials are higher than those in the other two electrolytes for different charge densities and obviously decrease with increasing f_i/f_j values. The largest error between the exact and approximate surface potentials is only 1% at f_i/f_j=100 and the charge density is as low as 0.044 C/m^2 (FIG. 4(a)), 0.001 C/m^2 (FIG. 4(b)) and 0.038 C/m^2 (FIG. 4(c)). The error is smaller than 5% when the surface charge density is larger than 0.027 C/m^2 (FIG. 4). Therefore, we can deduce that the analytical expressions of surface potential are valid since the surface charge densities of materials are larger than these values.

FIG. 5 shows that the effect of dielectric saturation on surface potential becomes important for the surface with high charge density (>0.3 C/m^2) and the difference of surface potentials increases with increasing charge density in the presence and absence of dielectric saturation. The effect of dielectric saturation obviously increases with increasing surface charge density both in 0.001 mol/L (FIG. 5(a)) and 0.1 mol/L (FIG. 5(b)). The surface potentials are underestimated in classical theories of double layer because the dielectric saturation effects for high surface charge density was not considered.

The effects of dielectric properties of medium on electric field strength increased with increasing surface charge density [28]. The surface charge density of many materials, such as clays and clay minerals [36], membrane [37, 38], liposomes, [4] metal oxides [39] and nano-TiO_2 [40], are in the range of 0.05−0.5 C/m^2, and the electric field strength can reach as high as 10^8-10^9 V/m. Therefore, the dielectric saturation can affect the surface potential to some extent.

Once the surface potential was obtained, the selectivity coefficient of binary ion exchange can be theoretically calculated by [33]:

$$K_{i/j} = \mathrm{e}^{-(\beta_i Z_i - \beta_j Z_j)F\varphi_0/(2RT)} \tag{30}$$

In Na-Mg exchange (*i.e.* 1:1+2:1 mixed electrolytes), the surface potential was calculated by using Eq.(29), thus the selectivity coefficient, $K_{Mg/Na}$, could be theoretically predicted. In this study, only Coulomb interac-

DOI:10.1063/1674-0068/cjcp1907132

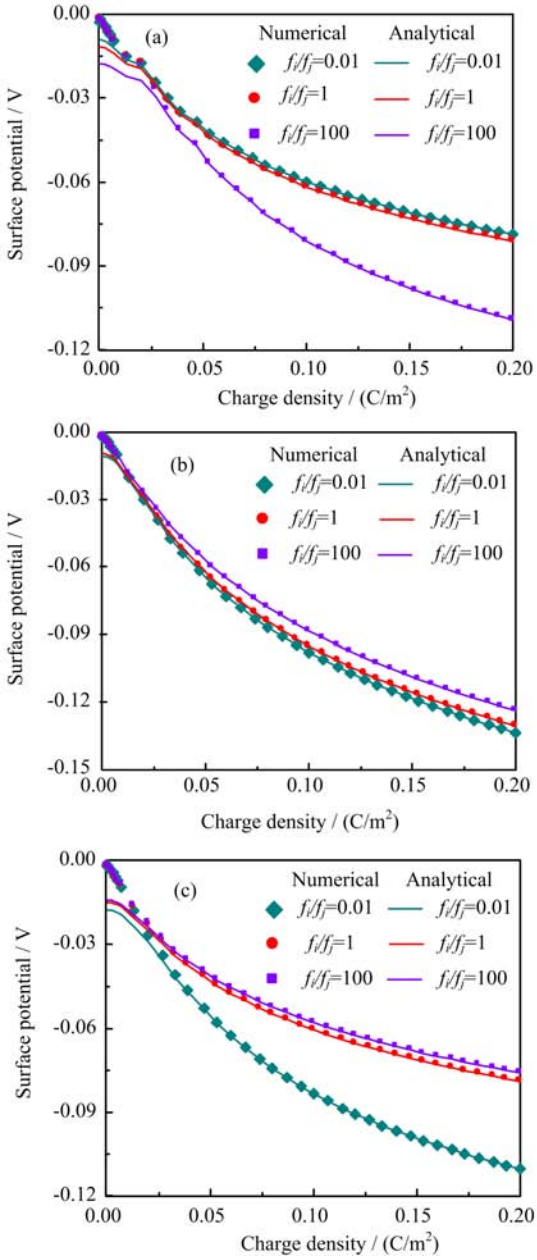

FIG. 4 The relationships between surface charge density and surface potential in (a) 1:1+2:2, (b) 1:1+1:2 and (c) 1:1+2:1 electrolyte solutions at different f_i/f_j values with ion strength of 0.1 mol/L. The symbols represent numerical surface potential and the solid lines represent analytical results.

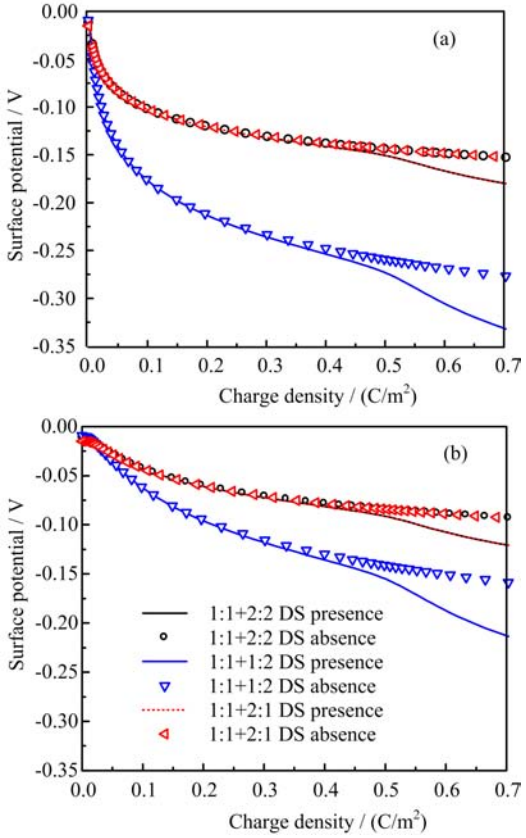

FIG. 5 The relationships between surface charge density and surface potential in the presence and absence of dielectric saturation. The ratio of bivalent ion concentration in mixed electrolytes is equal to 1, *i.e.* $f_i=f_j=f$, (a) f=0.001 mol/L and (b) f=0.1 mol/L. The solid lines and symbols represent the analytical surface potential in the presence and absence of dielectric saturation, respectively.

tion was considered, *i.e.* the effective charge coefficient β=1 for Mg^{2+} and Na^{+}. The predicted $K_{Mg/Na}$ for Altamont soil (the surface charge density is 0.6278 C/m^2 at pH=7 [41]) is in agreement with the experimental data [42] (FIG. 6). However, the classical PB description fails to predict the $K_{Mg/Na}$ calculated from the surface potential without considering the dielectric saturation (Eq.(19) or Eq.(20)) (FIG. 6).

In the present study, only dielectric saturation was taken into account in the surface potential determination based on the nonlinear PB equation of mean field approximation. The surface potential was underestimated compared with the determination by X-ray photoelectron spectroscopy [2] owing to the neglect of the hydrated cation size. Combining this and Brown's methods [2], the upcoming study will discuss the effects of dielectric saturation on the thickness of Stern layer. Furthermore, PB equation is highly approximate due to the neglect of ion-ion correlations [43], the solvent polarization and non-uniform size [44, 45], the ion polarizability [9, 10, 46, 47] and hydration [2, 48]. The charge reversal and charge amplification effects were observed in theoretical formalisms based on the model electrolytes composed by finit-sized ions [49−51]. However, Naji *et al.* [52] have reported the occurrence of charge reversal and charge amplification in the double layer of a point-like ions electrolyte when a non-uniform dielectric constant is considered. If the potential distribution in the double layer was described considering the dielectric saturation, the averaged cumulative

DOI:10.1063/1674-0068/cjcp1907132

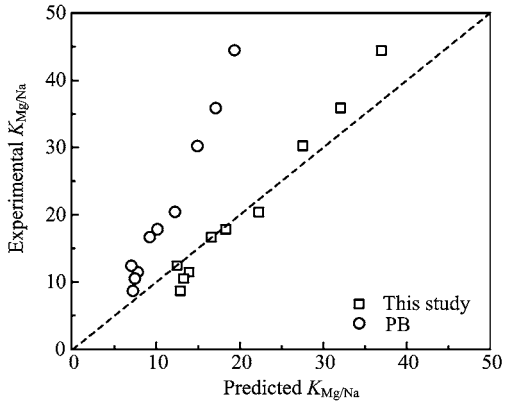

FIG. 6 Comparison between the experimental values and the predicted values of selectivity coefficient $K_{\mathrm{Mg/Na}}$ on Altamont soil. The experimental data were cited from Fletcher's work [42] and the dashed line is the 1:1 reference line.

charge can be calculated, and the charge reversal effect can be evaluated. These factors will be also taken into account to estimate the surface potential in subsequent studies.

V. CONCLUSION

A principle of surface potential determination of the charged particles in mixed electrolyte solutions was established considering the dielectric saturation. The analytical expressions of the surface potential with charge density were derived in different mixed electrolytes. As long as the surface charge density of nano/colloidal particles was known in advance, the dielectric constant and electric field strength at the particle surface can be calculated based on a nonlinear dielectric function of Langevin equation, and then the surface potential can be estimated using the established equations. Surface charge density is an important factor that affects the relative errors between analytical and numerical calculations of surface potentials and influences the effects of dielectric saturation. The approximate analytical expression can accurately evaluate the surface potential when surface charge density is higher than 0.044 $\mathrm{C/m^2}$ with errors smaller than 1% and 0.027 $\mathrm{C/m^2}$ with errors smaller than 5% in the ion strength of 0.001−0.1 mol/L, respectively. The ion strength and ratio of concentrations become important in exact numerical calculations only for very low surface charge densities.

VI. ACKNOWLEDGMENTS

This work was supported by the National Natural Science Foundation of China (No.41877026), the Natural Science Foundation Project of CQ CSTC (cstc2018jcyjAX0318) and the "Guangjiong" Project of Southwest University, China (201716).

[1] G. Trefalt, S. H. Behrens, and M. Borkovec, Langmuir **32**, 380 (2016).
[2] M. A. Brown, Z. Abbas, A. Kleibert, R. G. Green, A. Goel, S. May, and T. M. Squires, Phys. Rev. X **6**, 011007 (2016).
[3] E. C. Y. Yan, Y. Liu, and K. B. Eisenthal, J. Phys. Chem. B **102**, 6331 (1998).
[4] Y. Liu, E. C. Yan, X. Zhao, and K. B. Eisenthal, Langmuir **17**, 2063 (2001).
[5] H. Li, C. L. Qing, S. Q. Wei, and X. J. Jiang, J. Colloid Interface Sci. **275**, 172 (2004).
[6] J. Hou and H. Li, Soil Sci. Soc. Am. J. **73**, 1658 (2009).
[7] X. Liu, R. Tian, R. Li, W. Ding, H. Li, and R. Yuan, Proceedings A **471**, 20150064 (2015).
[8] P. F. Low, Soil Sci. Soc. Am. J. **45**, 1074 (1981).
[9] X. Liu, W. Ding, R. Tian, W. Du, and H. Li, Soil Sci. Soc. Am. J. **81**, 268 (2017).
[10] X. Liu, H. Li, R. Li, D. Xie, J. Ni, and L. Wu, Sci. Rep. **4**, 5047 (2014).
[11] M. C. F. Wander and A. E. Clark, J. Phys. Chem. C **112**, 19986 (2008).
[12] Y. Nakayama and D. Andelman, J. Chem. Phys. **142**, 044706 (2015).
[13] A. Gupta and H. A. Stone, Langmuir **34**, 11971 (2018).
[14] J. Peng, W. X. Zou, R. Tian, H. Li, and X. M. Liu, Chin. Phys. B **27**, 126801 (2018).
[15] R. L. Fulton, J. Chem. Phys **130**, 204503 (2009).
[16] D. L. Parkhurst and C. A. J. Appelo, *U.S. Geological Survey Techniques and Methods*, USGS, (2013).
[17] A. Abrashkin, D. Andelman, and H. Orland, Phys. Rev. Lett. **99**, 077801 (2007).
[18] D. C. Grahame, J. Chem. Phys. **18**, 903 (1950).
[19] G. H. Bolt, J. Colloid Sci. **10**, 206 (1955).
[20] L. Daniels, M. Scott, and Z. L. Mišković, J. Chem. Phys. **146**, 094101 (2017).
[21] D. Ben-Yaakov, D. Andelman, and R. Podgornik, J. Chem. Phys. **134**, 074705 (2011).
[22] N. Gavish and K. Promislow, Phys. Rev. E **94**, 023115 (2016).
[23] J. López-García, J. Horno, and C. Grosse, J. Colloid Interface Sci. **496**, 531 (2017).
[24] P. Hnenberger and M. Reif, S*ingle-Ion Solvation: Experimental and Theoretical Approaches to Elusive Thermodynamic Quantities*, Vol.3, Royal Society of Chemistry, 664 (2011).
[25] P. Sharma and Z. L. Mišković, Phys. Rev. B **90**, 125415 (2014).
[26] L. Daniels, M. Scott, and Z. L. Mišković, Chem. Phys. Lett. **701**, 43 (2018).
[27] Y. Uematsu, R. R. Netz, and D. J. Bonthuis, J. Phys.: Condens. Matter **30**, 064002 (2018).
[28] X. Liu, R. Tian, W. Du, R. Li, W. Ding, and H. Li, Appl. Clay Sci. **169**, 112 (2019).
[29] E. Gongadze, U. van Rienen, V. Kralj-Iglič, and A. Iglič, Gen. Physiol. Biophys. **30**, 130 (2011).
[30] S. Y. Mashayak and N. R. Aluru, J. Chem. Phys. **146**, 044108 (2017).

DOI:10.1063/1674-0068/cjcp1907132

[31] W. Ding, L. Xinmin, F. Hu, H. Zhu, Y. Luo, S. Li, and H. Li, J. Hydrol. **568**, 492 (2019).
[32] X. Liu, H. Li, W. Du, R. Tian, R. Li, and X. Jiang, J. Phys. Chem. C **117**, 62451 (2013).
[33] Y. T. Li, X. M. Liu, R. Tian, W. Q. Ding, W. N. Xiu, L. L. Tang, J. Zhang, and H. Li, Acta Phys. Chim. Sin. **33**, 1998 (2017).
[34] Y. Zhou, G. Stell, and H. L. Friedman, J. Chem. Phys. **89**, 3836 (1988).
[35] G. H. Bolt, Soil Sci. **79**, 267 (1955).
[36] H. Li, J. Hou, X. Liu, and L. Wu, Soil Sci. Soc. Am. J. **75**, 2128 (2011).
[37] H. Boroudjerdi, Y. W. Kim, A. Naji, R. R. Netz, X. Schlagberger, and A. Serr, Phys. Rep. **416**, 129 (2005).
[38] T. B. Kinraide and P. Wang, J. Exp. Bot. **61**, 2507 (2010).
[39] M. Mullet, P. Fievet, J. C. Reggiani, and J. Pagetti, J. Membr. Sci. **123**, 255 (1997).
[40] X. Liu, H. Li, R. Li, R. Tian, and C. Xu, Analyst **138**, 1122 (2013).
[41] S. Goldberg, S. M. Lesch, D. L. Suarez, and N. T. Basta, Soil Sci. Soc. Am. J. **69**, 1389 (2005).
[42] P. Fletcher, G. Sposito, and C. S. LeVesque, Soil Sci. Soc. Am. J. **48**, 1016 (1984).
[43] I. S. Sidhu, A. L. Frischknecht, and P. J. Atzberger, ACS Omega **3**, 11340 (2018).
[44] J. S. Sin, J. Chem. Phys. **147**, 214702 (2017).
[45] D. Shiby and E. Ruckenstein, Chem. Phys. Lett. **100**, 277 (1983).
[46] D. F. Parsons and B. W. Ninham, Langmuir **26**, 1816 (2010).
[47] D. Frydel, J. Chem. Phys. **134**, 234704 (2011).
[48] M. A. Brown, G. V. Bossa, and S. May, Langmuir **31**, 11477 (2015).
[49] M. Deserno, F. Jiménez-ángeles, C. Holm, and M. Lozada-Cassou, J. Phys. Chem. B **105**, 10983 (2001).
[50] F. Jiménez-ángeles and M. Lozada-Cassou, J. Phys. Chem. B **108**, 7286 (2004).
[51] G. I. Guerrero-García, E. González-Tovar, M. Chávez-Páez, and M. Lozada-Cassou, J. Chem. Phys. **132**, 054903 (2010).
[52] A. Naji, M. Ghodrat, H. Komaie-Moghaddam, and R. Podgornik, J. Chem. Phys. **141**, 174704 (2014).

DOI:10.1063/1674-0068/cjcp1907132